




## Article

# Geothermal Potential of the Brenner Base Tunnel—Initial Evaluations

Thomas Geisler <sup>1,\*</sup> , Klaus Voit <sup>2</sup> , Ulrich Burger <sup>3</sup>, Tobias Cordes <sup>3</sup>, Florian Lehner <sup>3</sup>, Gregor Götzl <sup>4</sup> , Magdalena Wolf <sup>5</sup> and Thomas Marcher <sup>1</sup>

<sup>1</sup> Institute of Rock Mechanics and Tunnelling, Graz University of Technology, 8010 Graz, Austria; thomas.marcher@tugraz.at

<sup>2</sup> Institute of Applied Geology, University of Natural Resources and Life Sciences, 1190 Vienna, Austria; klaus.voit@boku.ac.at

<sup>3</sup> Galleria di Base del Brennero—Brenner Basistunnel BBT SE, 6020 Innsbruck, Austria; ulrich.burger@bbt-se.com (U.B.); tobias.cordes@bbt-se.com (T.C.); florian.lehner@bbt-se.com (F.L.)

<sup>4</sup> Department of Hydrogeology and Geothermal Energy, Federal Geological Survey, 8010 Vienna, Austria; gregor.goetzl@geologie.ac.at

<sup>5</sup> Department of Material Sciences and Process Engineering, University of Natural Resources and Life Sciences, 1190 Vienna, Austria; magdalena.wolf@boku.ac.at

\* Correspondence: geisler@tugraz.at

**Abstract:** Increasing demands on mobility and transport, but limited space above ground, lead to new traffic routes being built, even more underground in the form of tunnels. In addition to improving the traffic situation, tunnels offer the possibility of contributing to climate-friendly heating by indirectly serving as geothermal power plants. In this study, the geothermal potential of the future longest railway tunnel in the world, the Brenner Base Tunnel, was evaluated. At the Brenner Base Tunnel, warm water naturally flows from the apex of the tunnel towards the city of Innsbruck, Austria. In order to estimate its geothermal potential, hydrological data of discharge rates and temperatures were investigated and analyzed. The investigations indicated the highest geothermal potential in the summertime, while the lowest occurs during winter. It could be shown that these variations were a result of cooling during discharge through areas of low overburden (mid mountain range), where the tunnel atmosphere is increasingly influenced by the air temperatures outside the tunnel. Nevertheless, the calculations showed that there will be a usable potential after completion of the tunnel.

**Keywords:** geothermal energy; water; sectional discharges; geothermal potential; tunnels; hydrology; water inflow



**Citation:** Geisler, T.; Voit, K.; Burger, U.; Cordes, T.; Lehner, F.; Götzl, G.; Wolf, M.; Marcher, T. Geothermal Potential of the Brenner Base Tunnel—Initial Evaluations. *Processes* **2022**, *10*, 972. <https://doi.org/10.3390/pr10050972>

Academic Editors: Edith Haslinger and Dejan Milenic

Received: 5 April 2022

Accepted: 9 May 2022

Published: 12 May 2022

**Publisher's Note:** MDPI stays neutral with regard to jurisdictional claims in published maps and institutional affiliations.



**Copyright:** © 2022 by the authors. Licensee MDPI, Basel, Switzerland. This article is an open access article distributed under the terms and conditions of the Creative Commons Attribution (CC BY) license (<https://creativecommons.org/licenses/by/4.0/>).

## 1. Introduction

In view of demographic changes and the growing demand for energy, future-oriented heat supply technologies, such as geothermal energy, are strategic. At the same time, due to limited available space and the current efforts to expand infrastructure networks, the construction of transport routes will increasingly shift underground. In addition, European transport corridors are currently being uniformly expanded to create a Trans-European Transport Network (TEN-T) for efficient and sustainable freight transport [1]. In order to comply with the Green Deal [2] demanded by the European Union and to minimize the impact of man-made climate change, a synergy of various climate-friendly, CO<sub>2</sub>-neutral technologies is required. An innovative contribution can be provided through the geothermal use of infrastructure projects. An example is the Brenner Base Tunnel (BBT), which is part of the European Corridor SCAN-MED [3]. Once construction is completed, the BBT will be the longest railway tunnel in the world, connecting Innsbruck in Tyrol, Austria, and Franzensfeste-Fortezza in South Tyrol, Italy (Figure 1) [4].

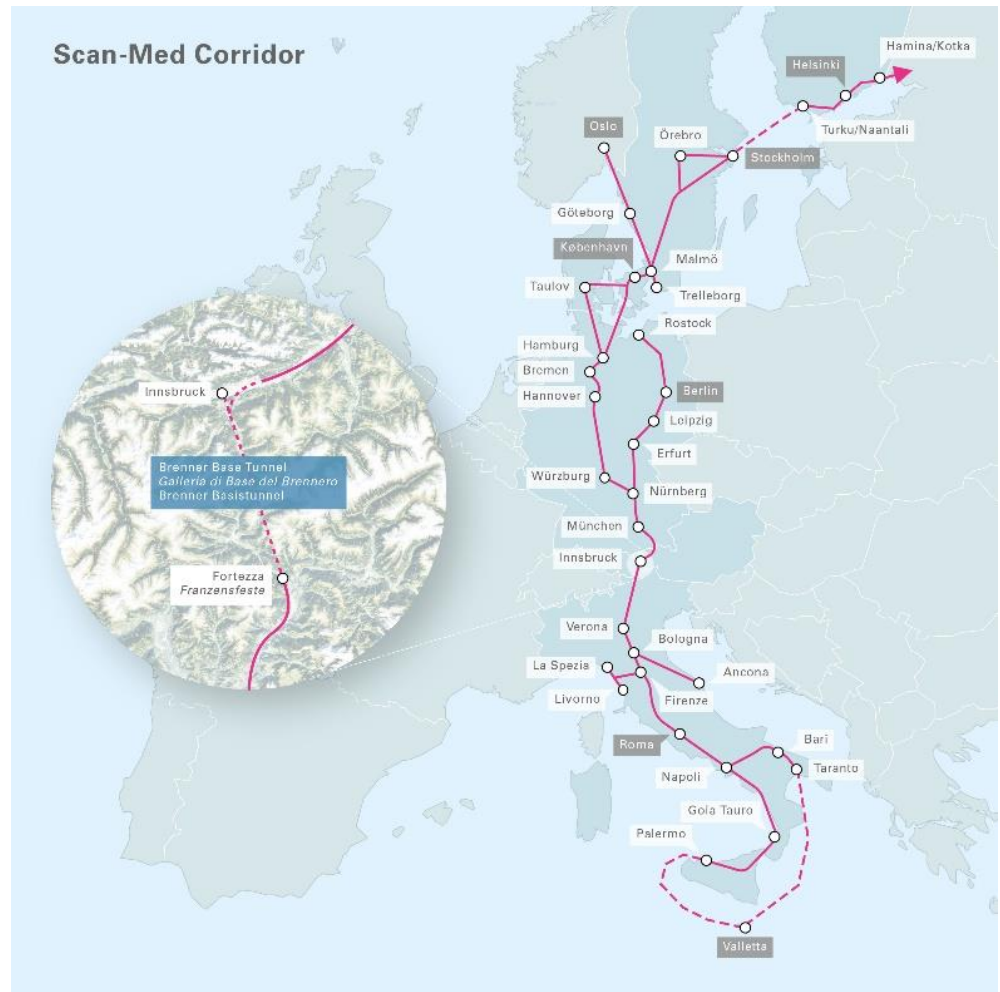


Figure 1. Location of the BBT, part of the Scandinavian–Mediterranean Corridor, for short Scan-Med Corridor, taken from [4].

On its path, the tunnel crosses different mountain ridges, valleys, and a complex crustal area in the alpine collision zone [5], with a maximum overburden of approximately 1700 m on the Italian side and approximately 1400 m on the Austrian side (Figure 2) [6].

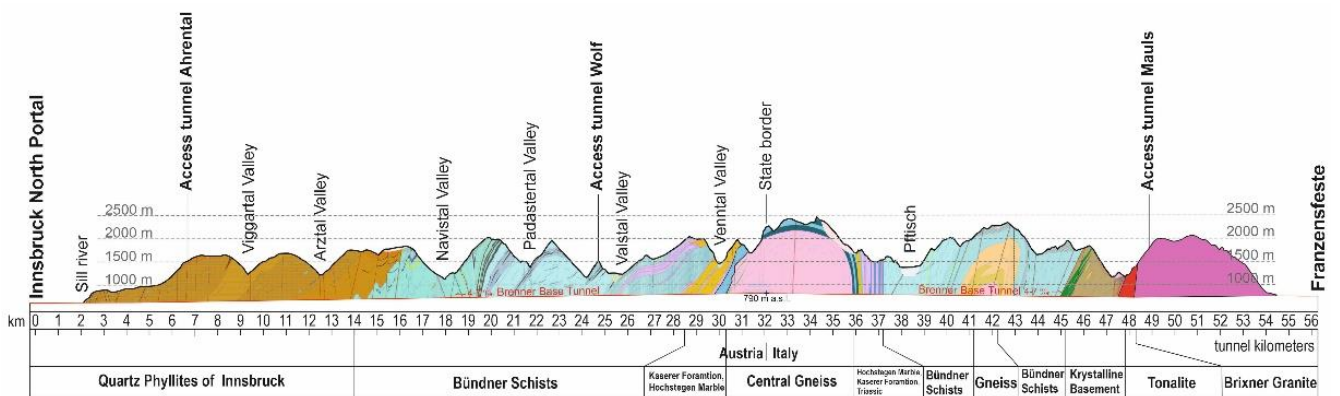


Figure 2. Geological longitudinal section of the Brenner Base Tunnel, modified from [7].

With an average geothermal gradient of 25 K/km, the rock mass temperature at the tunnel level reaches approx. 35 °C on the Austrian part. This heat can be extracted by components that are in contact with the ground [7], such as energy segments [8], energy geotextiles [9], and energy anchors [10]. As the construction progress of the BBT has been already started at the time of the presented research project, construction-related changes to the overall system are restricted. However, at the BBT, in addition to the use of geothermal energy from components in contact with the ground, drained and heated tunnel water is available. This warm water results from interactions with the rock mass through which it percolates [11]. As deep tunnels act as drainage, water may enter and accumulate during discharge on the way to the tunnel portal. At this point, the heat inherent in the tunnel water could then be extracted and transferred to a heating network. For the BBT, this might be applied at the northern portal at the Sill Gorge near Innsbruck, where it could be redistributed to consumers in Innsbruck (capital of Tyrol, Austria). The location at Sill Gorge would be optimal due to its proximity to the city of Innsbruck. Here, an efficient short-range heat transfer into a heating network with low forward temperatures would be practical.

Since at the BBT drained warm water could be used, it can be classified as an open hydrothermal tunnel system (HT). Currently, HT systems can be found in Central Europe, with the majority of them being established in Switzerland [12]. Thereby, an annual heat output of 5.3 GWh was generated in 2017 [13]. However, examples from Germany [14] and Austria [15] also show the magnitude of heat extraction from tunnels as well as the distribution to consumers [16,17].

This paper presents the results of the ThermoCluster project [18], funded by the Austrian Research Promotion Agency, aimed at evaluating the geothermal potential of the tunnel water of the BBT. An overview of the database and its further processing is presented together with the results and a discussion. Finally, an outlook of further research needs is presented.

## 2. Materials and Methods

### 2.1. The BBT Drainage System

The BBT consists of two main tunnel tubes, running about 70 m apart, and an exploratory tunnel (ET) about twelve meters, centrally below, to optimize the main tunnel drives during the construction phase (Figure 3). The entire tunnel system has a total length of 230 km, of which 151 km has already been excavated as of April 2022. Currently at the BBT, the excavation for ET and the access tunnels have already been completed for the most part as of March 2022. A distance of only about two kilometers still needs to be excavated to reach the national border at the Brenner Pass. In addition, the first parts of the main tunnels have already been excavated. During operation, the ET will serve as the service and drainage tunnel [19]. Thus, all water entering the tunnel system is drained through the ET to the tunnel portals, within the bottom channel of the invert segment. The apex of the tunnel system is located in the area of Brenner Pass at the national border between Austria to the north and Italy to the south. Therefore, water entering the 32 km long section on the Austrian part accumulates, mixes inside the tunnel, and discharges at the northern portal at Sill Gorge into the receiving watercourse, Sill River. Water entering the southern tunnel section flows to the southern portal to Franzensfeste-Fortezza. Thus, the geothermal potential at Sill Gorge is determined by water entering the northern tunnel section between Innsbruck and Brenner Pass [20].

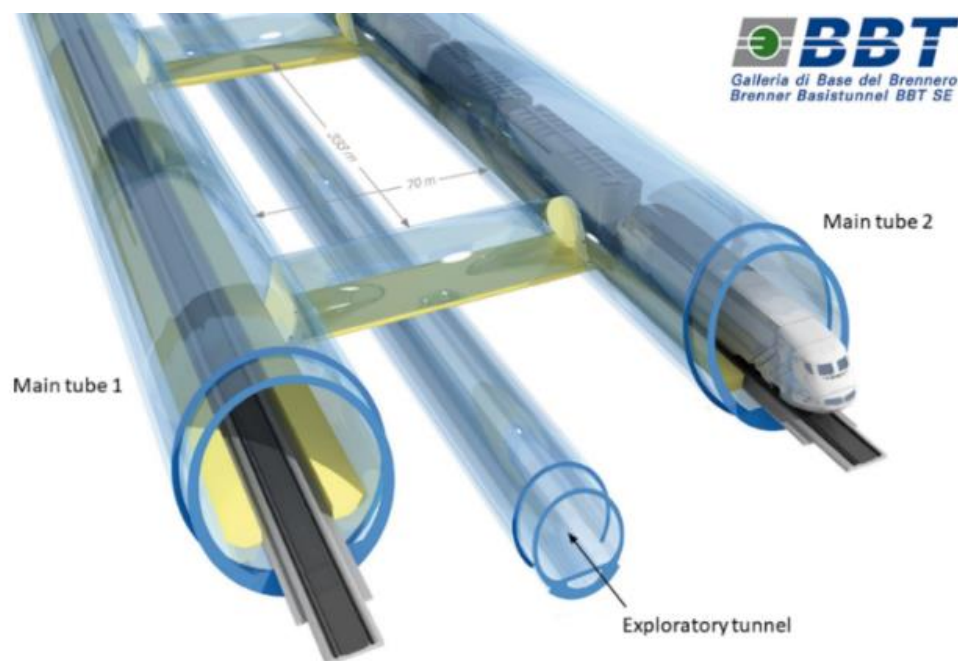


**Figure 3.** Sketch of the BBT cross section, modified from [21].

## 2.2. Data

To determine the thermal performance of the discharged water, two parameters are of particular importance, namely the discharge rate and the temperature of the fluid at the tunnel portal [16]. At the BBT, the concept of sectional discharges is applied in addition to many individual discharge measurements. Part of this concept is that tunnel sections with homogeneous hydrological conditions and therefore homogenous properties are clustered and considered as a unique system. A single cluster is thus called sectional discharge (Sd). Each of these is hydrologically monitored, including parameters of temperature and discharge rate [21]. These measurements form the basis for assessing the geothermal potential of the tunnel water. All water entering the BBT on the Austrian side will finally be discharged into Sill River in Sill Gorge near the city of Innsbruck (Figure 4). Hence, the sum of the sectional discharges, as well as their thermal characteristics, give the total water discharge ( $D_{\text{total}}$ ) and temperature ( $T_{\text{TW}}$ ). In total, the northern section of the Brenner Base Tunnel is divided into seven sectional discharges, which will contribute to the tunnel water outflow at Sill Gorge during operation (Table 1). However, before the data were evaluated, it was investigated whether the tunnel water shows a stable range of discharge rate and temperature over time, as the establishment of hydrological equilibria is time-dependent [22]. For this purpose, hydrographs of the single sectional discharges were analyzed.

**Table 1.** Overview of the sectional discharges.

Abbreviation	Name of Sectional Discharge
Sd1	Border—status of excavation work
Sd2	Access tunnel Wolf
Sd3	Assembly cavern
Sd4	Access tunnel Ahrental
Sd5	Emergency station
Sd6	Connection tunnel
Sd7	Diffuse water ingress
Tunnel water total ( $TW_{\text{tot}}$ )	Sill Gorge

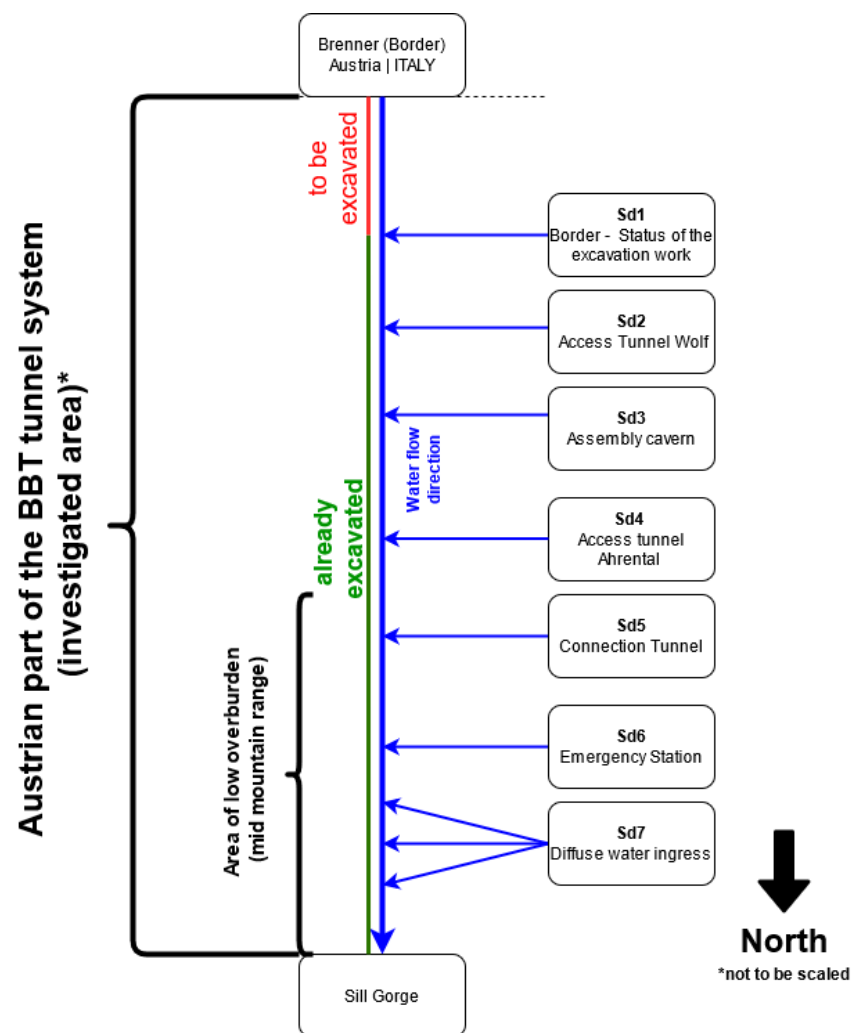


**Figure 4.** Tunnel water discharge system at the Austrian section of the BBT (\* not to be scaled).

### 2.3. Drainage System during Construction and Operational Phase

Brenner Base Tunnel is still under construction. The drainage system, and therefore the discharge rates and water temperatures differ significantly during the construction and operational phase. During construction, discharge rates are, to some extent, influenced by the excavation. Furthermore, temporary tunnel water redirections can lead to changes in the total amount of water discharged ( $D_{total}$ ) and the temperature ( $T_{TW}$ ). Therefore, data on the temperature and discharge rate of all sectional discharges were pre-processed and checked for plausibility. Moreover, for an adequate evaluation and estimation of the geothermal potential during the operational phase, the following aspects must be considered:

1. The southernmost part on the Austrian side of the ET (Sd1) has not yet been excavated; therefore, the quantities of water discharge and the temperature must be estimated in advance for this section. Prognoses, based on hydrogeological models, indicate ranges of 30–49 L/s and temperatures between 23–26 °C. Water from this hydrologically homogeneous area provides the greatest geothermal potential, since this section features the highest overburden on the Austrian side, combined with high water inflows.
2. Near the northern tunnel portal (between access tunnel Ahrental and Sill Gorge) there are several diffuse water inflows (Sd7), which cannot be measured directly. However, they are measured as part of the total water discharge at the Sill Gorge. Since the other sectional discharges contributing to the total water discharge are quantified, it is possible to determine the amount of diffuse inflows by subtracting the individual sectional discharges from the total water discharge. The diffuse inflows occur in



the area of a low overburden, from the northern tunnel portal to tunnel kilometer 6 (cf. Figure 2). These inflows represent the same hydrological regime as the sectional discharges Sd5 and Sd6. Therefore, the water temperatures are calculated using the average values of Sd5 and Sd6.

3. During the construction phase, Sd1 and Sd2, south of access tunnel Wolf—are not yet fed into the overall drainage system. The water of this construction lot is pumped back to the surface and discharged into the receiving water—the Upper Sill. When the BBT will be in operation, Sd1 and Sd2 will be directed into the main drainage system, which will considerably increase the total discharge rate of water. Therefore, in order to give a forecast of water discharge and temperature for the operational phase, Sd1 and Sd2 must be considered.
4. In the area of the Sill Gorge, the total amount of the tunnel discharge water and its temperature are measured. The measurement location is situated within the tunnel, yet rather close to the surface. Thus, temperatures inside the tunnel adjust according to the outside temperatures. Consequently, the air temperature within the tunnel can drop significantly, especially in wintertime, resulting in a cooling of tunnel water. Therefore, at least the monthly mean data should be used for valid calculations. After completion of the construction, the heat exchange of the tunnel water and the tunnel air will be reduced, as the drainage system will reach its final state. In this phase, all water will be discharged within the invert segment (bottom channel) (Figure 5) from the national border to into the Sill River. In addition, the flow velocity will increase due to higher quantities of water.
5. Once the main tunnels are excavated, the amount of water entering the tunnels will increase in the hydrographically homogeneous areas where the main tunnels is excavated. This is related to the increase in surface area through which water can enter the tunnel. This increase in the discharge rate is estimated by a factor of 1.1–1.3, based on experiences of the first excavated main tunnel sections.
6. Regarding the prognoses ranges of Sd1 and Sd3, two scenarios were elaborated. Scenario 1 is predicted on the premise that during the operational phase Sd1 will account for a discharge rate of 30 L/s and 23 °C. An increase in discharge by a factor of 1.1 is further assumed for Sd3, since the main tunnels are not yet excavated and therefore more water will enter the tunnel system. Scenario 2 assumes a contribution of Sd1 to the water discharge rate of 49 L/s and 26 °C during the operational phase. An increase in the discharge induced by the excavation of the main tunnels by a factor of 1.3 is taken for Sd3. These scenarios are the most probable, even if the exact discharge rate will depend on the success of necessary sealing works (cf. Section 3.2). Therefore, inflow volumes could also be significantly lower.

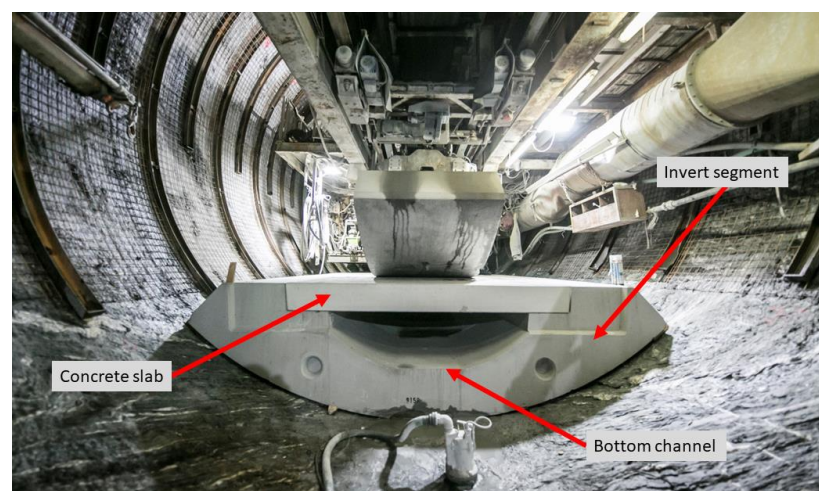


Figure 5. Invert segment with bottom channel and concrete slab (taken and modified from [6]).

Given these differences, the discharge rate ( $D_{tot}$ ) and its temperature ( $T_{total}$ ) during construction are defined by:

- Sd3
- Sd4
- Sd5
- Sd6
- Sd7
- Air temperature inside the tunnel in the area of the Sill Gorge

After completion, the discharge rate ( $D_{tot}$ ) and its temperature ( $T_{total}$ ) will be described by:

- Sd1 taken in Scenario 1 (30 L/s at 23 °C) or Scenario 2 (49 L/s at 26 °C) into account
- Sd2
- Sd3 taken in Scenario 1 (multiplied by 1.1) or Scenario 2 (multiplied by 1.3) into account
- Sd4
- Sd5
- Sd6
- Sd7
- Air temperature inside the tunnel area of Sill Gorge

The data for this study are measured values obtained from May 2020 to May 2021 to represent an entire year. Table 2 shows the expected mean discharge rates and mean temperatures of the individual sectional discharges contributing to the total tunnel water discharge after completion.

**Table 2.** Mean values of sectional discharges from May 2020 to May 2021 (\* estimated values). Bottom row shows total discharges and average temperature measured during excavation.

Sectional Discharge	Discharge Rate [L/s]	Temperature [°C]
Sd1 *	30–49	23–26
Sd2	15.0	12.2
Sd3	26.5	23.7
Sd4	5.4	16.3
Sd5	0.5	15.6
Sd6	2.5	14.7
Sd7	10.9	15.2
Total discharge ( $TW_{tot}$ )	45.8	17.8

#### 2.4. Cooling of the Tunnel Water in the Area of the Sill Gorge during Operational Phase

In the area of Sill Gorge, cooling of tunnel water occurs, caused by heat transfer of the warm tunnel water towards the colder tunnel air. To evaluate the magnitude of this cooling, the theoretical mixing temperature ( $T_{TWtheo}$ ) is calculated using Richmann's mixing rule [23]. The theoretical mixing temperature represents the temperature of the tunnel water while neglecting the influence of the tunnel air during the outflow towards the portal. The magnitude of cooling is represented by the delta ( $\Delta T$ ) of the theoretical mixed temperature and the actual measured temperature ( $T_{TWmeas}$ ), as the actual measured temperature includes the cooling induced by the outflow:

$$T_{TWtheo} - T_{TWmeas} = \Delta T \quad (1)$$

The heat emitted from tunnel water to ambient air during the construction phase is related to the temperature change,  $\Delta T$ , of the tunnel water. In order to obtain a reference value for the cooling, the heat transferred from the tunnel water to the tunnel air must be calculated. Since there is no phase change, the water heat content is:

$$Q = m \times c \times \Delta T \quad (2)$$

where  $Q$  represents the thermal energy (kJ),  $m$  is the mass of the fluid (kg) and  $c$  is the heat capacity of water (=4.183 J/(kg K) at 20 °C).

The heat energy emitted during the construction phase indicates a maximum value for the operating phase, since the water will have less opportunity to emit heat to the tunnel air. To calculate the maximum cooling of the tunnel water during the operational phase, the formula is rearranged according to  $\Delta T$ . The calculated  $Q$  and mass  $m$  of the water, which is to be expected during the operational phase, must be inserted. The recalculated  $\Delta T$  is subtracted from the theoretical mixing temperature during the operational phase. The result is the minimum temperature for the tunnel water during the operational phase.

### 2.5. Calculation of Heating Power of Tunnel Water

By knowing the tunnel water discharge ( $D_{total}$ ) and its temperature ( $T_{TW}$ ), it is possible to calculate the thermal power. Heating power  $P_{TW}$  is calculated [21,24] using:

$$P_{TW} = c \times \rho_{Water} \times D_{total} \times \Delta T_{TW} \quad (3)$$

where  $\rho_{Water}$  is the density of water and  $\Delta T_{TW}$  is the temperature spread ( $T_{TW} - T_0$ );  $T_0$  is the temperature to which the tunnel water is lowered.

The lowering temperature,  $\Delta T_{TW}$ , is controlled by two factors. On the one hand, by the heat extraction capacity of the heat exchanger, and, on the other hand, by the quantity and temperature of the tunnel water that is discharged into the receiving watercourse in compliance with environmental regulations [21]. For the calculation of the thermal power in this project, a cooling temperature ( $T_0$ ) of 10 °C is used, as the receiving Sill River has an average discharge rate of 26 m<sup>3</sup>/s and an average water temperature of 6.6 °C. Therefore, cooling of 10 °C might be acceptable, which, of course, needs to be investigated in more detail to not influence the receiving watercourse.

## 3. Results

### 3.1. Discharge Rates and Temperatures during the Construction Phase

Figure 6 shows the discharge rates and temperatures at the northern tunnel portal from May 2020 until May 2022. Discharge rates at the Sill Gorge portal decreased continuously over the period of May 2020–May 2021, from 49.1 to 40.0 L/s. In the period of May 2020–April 2021, one of the largest heat supply sections, in particular, Sd3, showed a continuous decrease until the discharge rate increased again in May 2021. The theoretical temperature calculated by Richmann's mixing rule showed the highest temperatures in August at 22.0 °C and the lowest temperatures in April at 18.7 °C. In the wintertime, from December to April, the temperature ranged between 19.7 °C and 18.7 °C. In the warmest months, the temperature varied from 22 °C to 20.1 °C.

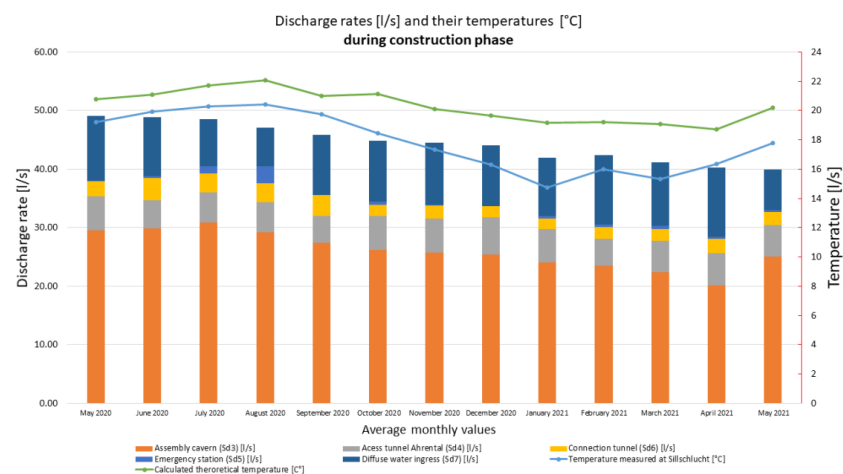


**Figure 6.** Discharge rates [L/s] (primary axis) in connection with the by the Richmann's mixing rule calculated theoretical (green line) and the measured (blue line) temperature [°C] at the northern portal of the BBT, Sill Gorge during construction.



Regarding the onsite measured temperature of the tunnel water it was observed that it varied from 20.4 °C in August to 14.7 °C in January. In the wintertime, from December to April, it displayed values between 16.3 °C and 14.7 °C.

The deviation (cooling of tunnel water during the discharge within the tunnel) of the measured temperature from the theoretically calculated temperature was largest in January at 4.4 °C, while it is lowest in June and September at 1.2 °C.

### 3.2. Discharge Rates and Their Temperatures during the Operational Phase

#### 3.2.1. Scenario 1

Figure 7 shows the prognosis for the operational phase of Scenario 1. It determines that the discharge rates vary between 96.4 L/s in September 2020 and 88.6 L/s in April 2021. Slightly higher discharge rates occur from September to December 2020. The theoretically highest temperature would occur in July at 21.6 °C, while the lowest would occur in December of the same year with 18.5 °C. The minimum temperature brought by cooling in the midmountain region would be highest in July, at 20.9 °C, while it would be lowest in December at 16.9 °C. The deviation of the theoretical to the minimum temperature is lowest in September at 0.6 °C, while it would be highest in January at 2.1 °C.

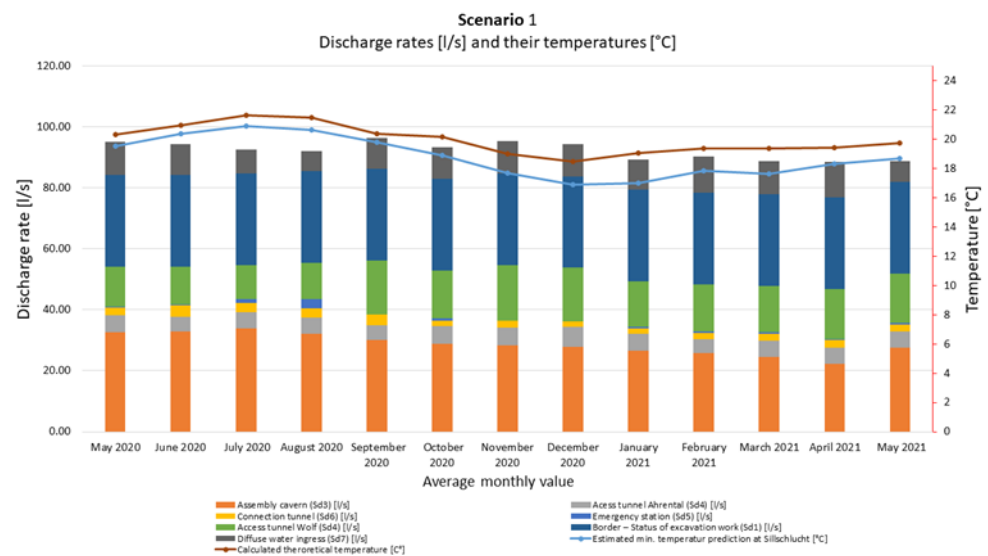


**Figure 7.** Discharge rates [L/s] (primary axis) in connection with the by the Richmann's mixing rule calculated theoretical (brown line) and the min. theoretical temperature (blue line) temperature [°C] at the northern portal of Innsbruck, Sill Gorge, during operation for Scenario 1.

#### 3.2.2. Scenario 2

Figure 8 displays Scenario 2. The discharge rate would be highest in September 2020 at 120.9 L/s and lowest in April 2021 at 111.6 L/s. Again, slightly higher discharge rates would be present during the months of September to December. The theoretically highest temperatures would appear in July at 23.2 °C, while the minimum would occur in December at 20.6 °C. The calculated minimum temperature would be lowest in December with 19.4 °C and highest at 22.6 °C in July. The deviation of the theoretical temperature and the temperature influenced by cooling would be highest in January at 1.6 °C and lowest in September at 0.5 °C.

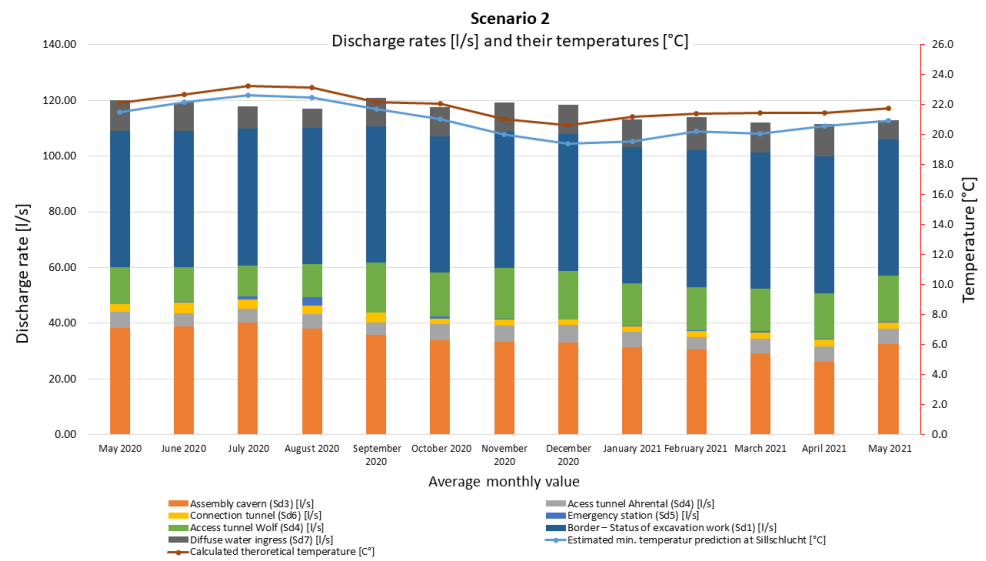


**Figure 8.** Discharge rates [L/s] (primary axis) in connection with the by the Richmann’s mixing rule calculated theoretical (brown line) and the min. theoretical temperature (blue line) temperature [°C] at the northern portal of Innsbruck, Sill Gorge during operation for Scenario 2.

### 3.3. The Predicted Geothermal Potential after Completion of the BBT

Figures 9 and 10 show the geothermal power calculated by means of Equation (3) for Scenarios 1 and 2 and indicating that the heating power is higher when considering the theoretical mixing temperatures. On an annual average, it is 0.45 MW higher than the heating power calculated on the minimum temperatures. The highest deviation is therefore observed in January with 0.78 MW, while the lowest occurs in June at 0.24 MW. For Scenario 1 (Figure 9), the highest power is expected in July and ranges between a maximum value of 4.50–4.21 MW. The lowest thermal power is expected in December and January with 2.61–3.34 MW. Scenario 2 (Figure 10) also displays that the highest power is expected in July and ranges between a maximum value of 6.52 MW–6.23 MW. The lowest thermal power is expected in December and January with 4.54–5.27 MW and the highest also in July with 6.22–6.51 MW.

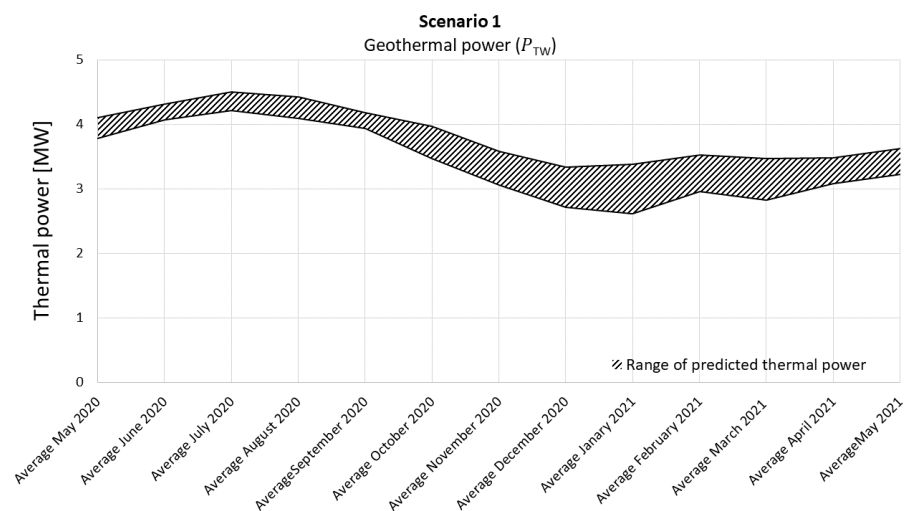


**Figure 9.** Range of possible thermal power [MW], which might be available during the operational phase of the tunnel for Scenario 1.

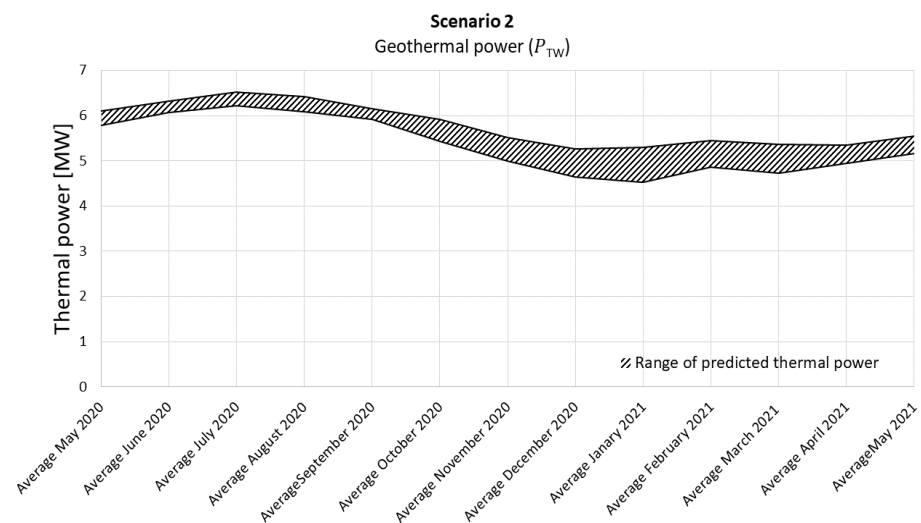


**Figure 10.** Range of possible thermal power [MW], which might be available during the operational phase of the tunnel for Scenario 2.

### 3.4. Interpretation

#### 3.4.1. Total Tunnel Water Discharges and Temperatures during Construction

Within the period May 2020–April 2021, a decrease in the total tunnel water discharge rate was observed. This decrease of discharge rate resulted from Sd3, whereas the other contributing sectional discharges indicated minor seasonal variations. Sd3 discharge rate showed a slight decrease until April 2021 as in May 2021, the discharge rate of Sd3 increased to 25 L/s. The change of discharge rate in Sd3 is related to the transition from transient to stationary flow conditions of the major water inflows on the one hand and to the complex hydrogeological boundary conditions in the area on the other. However, the comparison of the theoretical tunnel water mixing temperatures and the temperature recorded at the tunnel portal in Sill Gorge reveals a high discrepancy ( $\Delta T$ ) (Figure 6). The measured tunnel water temperature is lower than the theoretically determined temperature. This observed discrepancy arises as the theoretically calculated temperatures do not include cooling or heating of the tunnel water during discharge, while the measured temperatures already account for them. Therefore, cooling occurs during the outflow, as the tunnel air temperature is lower than the tunnel water temperature. Since the northernmost area of the BBT has a low overburden (cf. Figure 3) and due to the open portal enabling air circulating inside the northernmost tunnel section, the rock mass temperatures and, thus, the tunnel air temperature are lower than in the sections with higher overburden. The highest deviation of the theoretically calculated tunnel water temperature from the measured temperature is observed in December and January. During these months, the average air temperature of the city of Innsbruck (measured at the University of Innsbruck, close to the Portal Sill Gorge) is  $-0.5\text{ }^{\circ}\text{C}$  in January and  $1.8\text{ }^{\circ}\text{C}$  in December [25]. The difference of the theoretically calculated tunnel water temperature (approx.  $19.5\text{ }^{\circ}\text{C}$ ) and the tunnel air adapting to the outside temperatures should be about  $18.5\text{ }^{\circ}\text{C}$  during the construction phase, thus producing cooling in the wintertime. In the summertime, this deviation and therefore the natural convection is reduced, due to higher temperatures outside the tunnel.

#### 3.4.2. Total Tunnel Water Discharges and Temperature Predictions during Operation

Except for Sd1 and Sd3, all sectional discharges that will determine the future discharge are based on observed values. During the operational phase, Sd1 and Sd3 will significantly contribute to the total discharge but their amounts are subject to uncertainties. Although for Sd1 forecasts for the discharge rate and temperatures are available, this section contains hydrological uncertainties, which is why these forecasts are expressed in a bandwidth. One

reason for the given range is, that in the section of Sd1 rock sealing works will reduce the hydraulic permeability of the rock mass as they will be essential to ensure a safe tunnel excavation. The rock sealing techniques in this tunnel section will mainly be in the form of grout injections and will reduce the water ingress to a minimum, and sustain the shallow original water levels in this region. The specified bandwidth thus reflects the predicted amount of water.

Another uncertainty is the discharge rate increase induced by the excavation of the main tunnels affecting Sd3. At the present status of excavation, it is not possible to specify the exact factor by which Sd3 will increase. Sd3 is the largest heat energy supplier after Sd1, thus its discharge rate and temperature have a huge impact on the total discharge rate at the northern tunnel portal at the Sill Gorge.

Moreover, cooling of the tunnel water in the area of Sill Gorge (area of low overburden) will also occur during the operational phase. The calculation of the maximum cooling during operation in the area of Sill Gorge, respectively in the area with low overburden, is based on the expectation that the tunnel water cannot release more energy during the operating phase than the construction phase. Assuming all conditions remain the same (tunnel air temperatures, tunnel water flow velocity, etc.), the difference of the theoretical tunnel water temperature from the actual future tunnel water temperature will however decrease as the result of the larger water mass ( $\Delta T$ ). As the mass and therefore the volume of the tunnel water increases during the operational phase, the cross section of the bottom channel remains the same. This leads to an increased flow velocity. Consequently, the water has less time to adapt to the temperature of the tunnel air. As a result, the cooling is reduced, through which the predicted minimum temperature and the theoretical temperature further converge. In addition, future tunnel ventilation will have an effect on the final discharge temperature, since the temperature inside the tunnel is influenced by the ventilation. The magnitude of influence resulting from tunnel ventilation cannot be estimated at this stage.

### 3.4.3. Geothermal Power of the BBT Tunnel Water

To represent bandwidths brought by prognosis uncertainties of Sd1 and Sd3, two scenarios were presented. In principle, the higher the water discharge and water temperature, the higher the thermal output. Since according to Scenario 2 a higher discharge rate in combination with higher temperatures are predicted, Scenario 2 represents the optimal and Scenario 1 the suboptimal case. However, the calculations of the geothermal potential assume that the tunnel water is cooled down to 10 °C. A further cooling of the temperature leads to a wider span of the applicable temperature range. This would increase the output considerably as shown in Figures 9 and 10, since the upper end of the range is calculated based on the theoretical mixing temperatures, while the lower end is calculated using the post-cooling temperatures. Both Scenarios 1 and 2 show that the lowest thermal power will be available in the winter. Due to the stronger cooling of the water in the winter, the range of the predicted thermal power increases before decreasing in the summer months. Figures 9 and 10 also show how a supposedly small temperature difference affects thermal performance. For example, in Scenario 2 the thermal power in July is 6.37 MW at 22.9 °C and 117.8 L/s. In January, the thermal power is 4.91 MW at 19.8 °C and 113.12 L/s.

## 4. Discussion and Conclusions

When considering the calculated energy quantities (or the discharge rates as well as the water temperatures), it is evident that there are still some uncertainties which will be clarified in the course of the construction progress. Despite these uncertainties, the results show significant geothermal potential inherent in the BBT water. After completion of excavation of the last tunnel section to the national border (Sd1), the main prognosis uncertainty will be eliminated, and the range of the potential can be refined further. From this point on, it is recommended to work with numerical modeling regarding the cooling effect after construction is finished.

However, the geothermal potential is expected to be somewhere between Scenarios 1 and 2, whereby the impact of the necessary sealing work in section Sd1 is difficult to estimate. Once the tunnel will be in operation, it can be assumed that the cooling of the tunnel water in the area of Sill Gorge will continue to decrease and the tunnel water temperatures approach the theoretically calculated temperatures. The increase of the flow velocity leads to a reduced adaptation time for the water to the tunnel air temperature. Secondly, the interaction with the outside air will be reduced and thus the cooling minimized, especially during the wintertime. In addition, except for the last section with a lower overburden, the air temperatures are occasionally higher than the theoretically calculated temperatures of the tunnel water, which would result in a warming of the tunnel water in these sections. Nevertheless, this study also shows that the geothermal potential is very sensitive even to small variations in temperature. Therefore, the waterways should be isolated as much as possible, at least in the area with low overburden, where cooling occurs. Moreover, it should be noted that the temperatures obtained from the tunnel are significantly lower than the temperatures prevailing in a conventional district heating network [26].

At the BBT, the application of the system of sectional discharges and the detailed monitoring provides the basis for estimating the geothermal potential, although forecasting of the water inflow into a tunnel is a highly complicated task [27]. The broad data base presented in this study enables the possibility to give initial assessments several years before the construction work is completed. Hence, the application of the system of sectional discharges is an opportunity for the evaluation other tunnels as well. Further, the data enables an optimization at an early stage or an adaptation of the monitoring at certain points. These optimizations can be achieved by means of separate discharges of cold water inflows or by a subsequent installation of heat absorbers inside the tunnel. These absorbers could be installed in areas of high overburden and thus high rock mass temperatures. Using absorbers could additionally heat the water and increase its temperature at the tunnel portal.

It can be concluded that the geothermal use of the BBT could contribute as an added value to the benefits yield by this new infrastructure of the European transportation system.

**Author Contributions:** Conceptualization, T.G.; data curation, U.B. and F.L.; formal analysis, T.G.; funding acquisition, T.G.; methodology, T.G. and G.G.; project administration, T.G.; supervision, T.M.; validation, K.V., U.B. and T.C.; visualization, T.G.; writing—original draft, T.G.; writing—review and editing, T.G., K.V., T.C., G.G. and M.W. All authors have read and agreed to the published version of the manuscript.

**Funding:** This research was funded by Austrian Research Promotion Agency, “879458” and the APC was funded by TU Graz Open Access Publishing Fund.

**Institutional Review Board Statement:** Not applicable.

**Informed Consent Statement:** Not applicable.

**Data Availability Statement:** Not applicable.

**Acknowledgments:** A special thanks for the realization of the study has to go to the whole Thermo-Cluster Team. The APC was funded by TU Graz Open Access Publishing Fund.

**Conflicts of Interest:** The authors declare no conflict of interest.

## References

1. European Parliament. Decision No 1692/96/EC of the European Parliament and of the Council of 23 July 1996 on Community Guidelines for the Development of the Trans-European Transport Network. 31996D1692. 1996, pp. 1–104. Available online: [http://publications.europa.eu/resource/cellar/f34131d1-aae6-4421-8394-c1cd130a4ed5.0006.02/DOC\\_1](http://publications.europa.eu/resource/cellar/f34131d1-aae6-4421-8394-c1cd130a4ed5.0006.02/DOC_1) (accessed on 2 April 2022).
2. Communication from the Commission to the European Parliament, the European Council, the Council, the European Economic and Social Committee and the Committee of the Regions: The European Green Deal. Available online: <https://eur-lex.europa.eu/legal-content/EN/TXT/?uri=COM%3A2019%3A640%3AFIN> (accessed on 2 April 2022).



3. Tinti, F.; Boldini, D.; Ferrari, M.; Lanconelli, M.; Kasmaee, S.; Bruno, R.; Egger, H.; Voza, A.; Zurlo, R. Exploitation of geothermal energy using tunnel lining technology in a mountain environment. A feasibility study for the Brenner Base tunnel–BBT. *Tunn. Undergr. Space Technol.* **2017**, *70*, 182–203. [CrossRef]
4. BBT-SE. Europäisch Dimension. Available online: <https://www.bbt-se.com/tunnel/europaeische-dimension/> (accessed on 27 April 2022).
5. Brandner, R.; Reiter, F.; Töchterle, A. Überblick zu den Ergebnissen der geologischen Vorerkundung für den Brenner-Basistunnel. *Geo. Alp* **2008**, *5*, 165–174.
6. Voit, K.; Kuschel, E. Rock Material Recycling in Tunnel Engineering. *Appl. Sci.* **2020**, *10*, 2722. [CrossRef]
7. Adam, D.; Markiewicz, R.; Oberhauser, A. Nachhaltige Nutzung von Erdwärme mittels innovativer Systeme im Ingenieurtiefbau und Tunnelbau. In *Ernst & Sohn Verlag (Hrsg.), 1*; Department für Bautechnik und Naturgefahren: Wien, Austria; pp. 113–117.
8. Pralle, N.; Friedemann, W.; Mayer, P.-M.; Grübl, F.; Ostermeier, B.; Schneider, M. Wärme lieferndes Fertigteil, Energietübbing. 12 September 2007. Available online: <https://patentimages.storage.googleapis.com/8d/ea/70/5f9ba66b399d73/EP1905947A1.pdf> (accessed on 12 March 2022).
9. Markiewicz, R. Numerische und Experimentelle Untersuchungen zur Nutzung von Geothermischer Energie Mittels Erdberührter Bauteile und Neuentwicklungen für den Tunnelbau. Ph.D. Dissertation, Technische Universität Wien, Wien, Austria, 2004.
10. Oberhauser, A.; Adam, D.; Hosp, M.; Kopf, F. Der Energieanker–Synergien bei der Nutzung eines statisch konstruktiven Bauteils. *Oesterreichische Ing.-Z.* **2006**, *151*, 97–102.
11. Rybach, L. Thermal waters in deep Alpine tunnels. *Geothermics* **1995**, *24*, 631–637. [CrossRef]
12. Stemmle, R.; Menberg, K.; Rybach, L.; Blum, P. Tunnelgeothermie – Ein Überblick. *Geomechanik und Tunnelbau* **2022**, *15*, 104–111. [CrossRef]
13. Buhmann, P.; Blossfeld, J.; Moormann, C. Geothermische Bergwassernutzung–Hydrogeothermische Verfahren an deutschen Straßentunneln. In *Fachsektionstage Geotechnik, Interdisziplinäres Forum*; Deutsche Gesellschaft für Geotechnik: Essen, Germany, 2017.
14. Moormann, C. GeoTU6—a geothermal Research Project for Tunnels. *Tunnel* **2010**, *29*, 14–21.
15. Adam, D.; Markiewicz, R. Energy from earth-coupled structures, foundations, tunnels and sewers. *Géotechnique* **2009**, *59*, 229–236. [CrossRef]
16. Rybach, L. Geothermal use of warm tunnel waters—Principles and examples from Switzerland. *Trans. Geotherm. Resour. Counc.* **2010**, *34*, 871–874.
17. Geisler, T.; Wolf, M.; Burger, U.; Voit, K.; Götzl, G.; Lauermaier, M.; Haslinger, E.; Auer, R.; Straka, W.; Pol, O.; et al. Geothermal Potential of infrastructure projects using the example of the Brenner base tunnel and the utilization of low-temperature heat in urban regions. Vienna. In Proceedings of the 13th International Conference on Sustainable Energy & Environmental Protection, Vienna, Austria, 13–16 September 2021; Volume 1, pp. 457–463.
18. Geisler, T.; Wolf, M.; Götzl, G.; Burger, U.; Cordes, T.; Pol, O.; Obradovic, M.; Straka, W.; Voit, K.; Haslinger, E.; et al. ThermoCluster: Wärmegewinnung aus Infrastrukturprojekten und Einbindung in Dezentrale Niedertemperatur-Wärme- und Kältenetze für Plus-Energie-Quartiere. (To Be Published). 2022. Available online: <https://projekte.ffg.at/projekt/3793907> (accessed on 15 March 2022).
19. Bergmeister, K.; Reinhold, C. Learning and optimization from the exploratory tunnel–Brenner Base Tunnel. *Geomech. Tunn.* **2017**, *10*, 467–476. [CrossRef]
20. BBT-SE. Mediathek. Available online: <https://www.bbt-se.com/information/mediathek/#&gid=1&pid=18> (accessed on 22 March 2022).
21. Burger, U.; Geisler, T.; Lehner, F.; Cordes, T.; Marcher, T. Sectional discharges as geothermal potentials of deep tunnels. *Geomech. Tunn.* **2022**, *15*, 92–103. [CrossRef]
22. Perello, P.; Baietto, A.; Burger, U.; Skuk, S. Excavation of the Aica-Mules pilot tunnel for the Brenner base tunnel: Information gained on water inflows in tunnels in granitic massifs. *Rock Mech. Rock Eng.* **2014**, *47*, 1049–1071. [CrossRef]
23. Richmann, G.W. De quantitate caloris, quae post miscelam flvidorum, certo gradv calidorum, oriri debet, cogitationes, avctore. *Typis Acad. Sci.* **1750**, *1*, 152–167.
24. Wilhelm, J.; Rybach, L. The geothermal potential of Swiss Alpine tunnels. *Geothermics* **2003**, *32*, 557–568. [CrossRef]
25. Klimamonitoring—ZAMG. Available online: <https://www.zamg.ac.at/cms/de/klima/klima-aktuell/klimamonitoring/?station=11803&param=t&period=period-ym-2020-12&ref=3> (accessed on 4 February 2022).
26. Buffa, S.; Cozzini, M.; D’Antoni, M.; Baratieri, M.; Fedrizzi, R. 5th generation district heating and cooling systems: A review of existing cases in Europe. *Renew. Sustain. Energy Rev.* **2019**, *104*, 504–522. [CrossRef]
27. Tentschert, E. Water Prediction for Tunnels—A Game of Chance? *Beitr. Zu Hydrogeologie* **2012**, *52*, 161–168.